ACS APPLIED NANO MATERIALS
Cite This: ACS Appl. Nano Mater. 2020, 3, 969−976
Forum Article
www.acsanm.org

3D-Printed Photoactive Semiconducting Nanowire−Polymer Composites for Light Sensors

Xin Shan,[†] Pengsu Mao,[†] Haoran Li,[†] Thomas Geske,[‡] Divya Bahadur,[§] Yan Xin,[∥] Subramanian Ramakrishnan,[§] and Zhibin Yu*[,†,‡]

[†]Department of Industrial and Manufacturing Engineering, High-Performance Materials Institute, FAMU-FSU College of Engineering, [‡]Materials Science and Engineering, [§]Department of Chemical and Biomedical Engineering, FAMU-FSU College of Engineering, and [∥]National High Magnetic Field Laboratory, Florida State University, Tallahassee, Florida 32310, United States

Supporting Information

ABSTRACT: We demonstrated 3D-printed photoactive composites for light sensors. The composites consist of semiconducting polymer nanowires dispersed in an insulating polymer matrix through a thermo- or photocuring process. The nanowires formed percolated networks for charge-carrier collection at a very low nanowire volume concentration. Photodetectors had been fabricated with such composites and obtained a low leakage current density of 25 nA cm^{-2}, a large conductivity change of 18025 times upon light irradiation (1 sun), and a high specific detectivity of 4.5×10^{10} Jones. The composite precursors before curing had been used as paints on different surfaces including wood, cardboard, and glass fiber cloth to create photoactive coatings on these surfaces. The precursors had also been used for 3D printing to create photoactive structures with a mechanical modulus of 4 GPa and an ultimate strength of 36 MPa.

KEYWORDS: *3D printing, composite, semiconductor, photodetector, P3HT, nanowire*

INTRODUCTION

Polymer-based composites have been widely used as structural components in the automotive, construction, and aerospace industries because of their ease of manufacturing and relatively high specific moduli and strengths.[1−3] With the adoption of additive manufacturing technologies, such composites can now be directly printed into complex 3D geometries with a high spatial resolution that is challenging with conventional molding and extrusion manufacturing processes.[4−6] In addition to enhancing their mechanical properties, the use of compositing can further introduce new electrical, photonic, or magnetic functionalities for the simultaneous monitoring of both the internal damage and surrounding environment changes of the composites and resulting structures.[7−11] Such information is paramount for assessing the health conditions of the composites and structures throughout their service lifespan.

The 3D printing of multifunctional polymer composites has been mostly focused on the use of conductive or insulating polymer composites, and the use of semiconducting composites has seldom been studied.[12] Semiconducting materials exhibit uniquely suited optoelectronic properties, potentially leading to more accurate real-time measurements of stress, strain, temperature, etc., with less energy and power consumption than their metallic and insulating counterparts.[13] In addition, the judicious selection of semiconducting materials can enable new composites and structures for the sensing of certain desired spectra of electromagnetic radiation, which is difficult to achieve if metallic or insulating composites are used.[14]

In this work, we report semiconducting nanowire−polymer composites and demonstrate their application as photoactive coatings and 3D-printed structures that sense visible light. The composites were prepared by dispersing semiconducting polymer nanowires into epoxy or acrylic resins, followed by curing with heat or UV light. The high aspect ratio of the embedded nanowires led to percolated network formation, and photocurrent was observed at a very low nanowire concentration of 0.1 wt %. The composites with about 2 wt % nanowires can have 18025 times more conductivity increase under 1 sun simulated solar-light irradiation. The nanowire−polymer composites also exhibit superior processability. Photoactive coatings can be formed on wood, cardboard, and glass fiber cloth through painting. The composites can also be 3D-printed to form 3D photoactive structures with high mechanical moduli and strengths. The printed structures can

Special Issue: Young Investigator Forum

Received: September 14, 2019
Accepted: December 11, 2019
Published: December 26, 2019

DOI: 10.1021/acsanm.9b01763
ACS Appl. Nano Mater. 2020, 3, 969−976

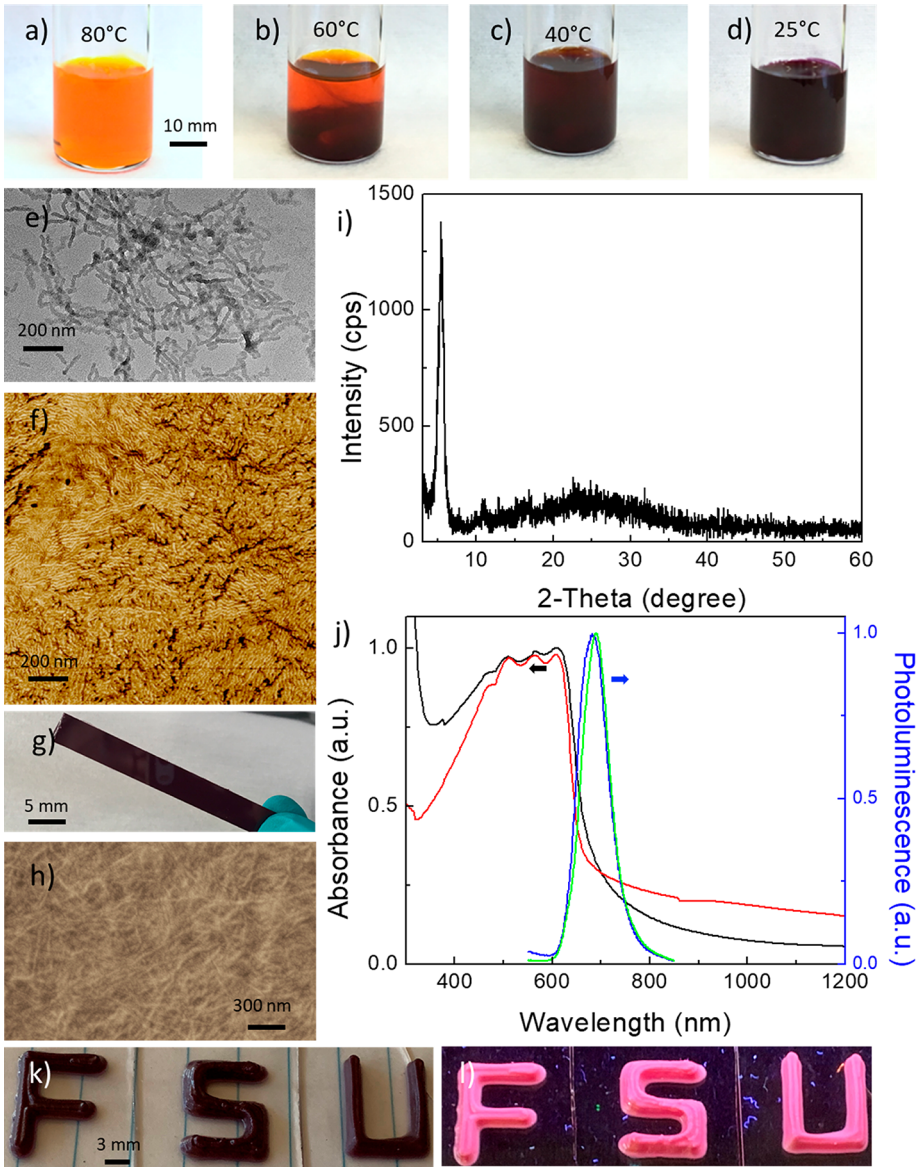

Figure 1. (a–d) Photographs showing the P3HT nanowire growth progression while cooling a homogeneous P3HT/DCM solution from 80 to 25 °C in a sealed glass vial. (e) TEM and (f) AFM images of the as-synthesized P3HT nanowires. (g) Photograph, (h) SEM image, (i) XRD pattern, and (j) absorbance (black) and PL (blue) spectra of one P3HT–epoxy composite with 1.96 wt % P3HT nanowires and absorbance (red) and PL (green) spectra of one standalone P3HT nanowire film. (k and l) Photographs of one 3D-printed "FSU" pattern in ambient light and under 365 nm UV light, respectively.

maintain their as-printed size and shape after curing of the resins because no solvents are used in the printing ink.

Poly(3-hexylthiophene-2,5-diyl) (P3HT) was used to prepare the photoactive composites in our study. P3HT has been extensively investigated for solar cells and photodetectors because of its relatively high charge-carrier mobility, high absorption to visible light, and good solubility in certain organic solvents.[15] For those applications, P3HT thin films of sub-100 nm to a few micrometers were used and fabricated by a solution-based spin-coating, inkjet-printing, or screen-printing process. Such processing methods are planar processes, which cannot be applied to form 3D bulk P3HT structures; moreover, the intrinsic mechanical properties and high material cost of P3HT are not ideal for load-bearing structure applications. To solve such problems, we investigated P3HT nanowire–polymer composites, where the optoelectronic properties of the composites came from P3HT nanowires, which formed an interconnected network in the composites and acted as charge-transport media for collection of the photogenerated charge carriers. The mechanical properties and processing techniques of the composites were determined by the matrix polymer because the incorporated P3HT had a relatively low volume concentration.

EXPERIMENTAL SECTION

Materials. Poly(3-hexylthiophene-2,5-diyl) (P3HT; regioregular, 58K molecular weight) was purchased from Rieke Metals. EPON Resin 862 (diglycidyl ether of bisphenol F) and EPIKURE Curing Agent W System (aromatic amine) were obtained from HEXION. Bisphenol A ethoxylate diacrylate (average $M_n \sim 512$, EO/phenol 2), 2,2-dimethoxy-2-phenylacetophenone (photoinitiator), dichloromethane, and indium–gallium eutectic (In–Ga) were purchased from Sigma-Aldrich. Dry cellulose nanofibers (CNFs) were purchased from the Process Development Center, University of Maine. All materials were used as received. The chemical structures of P3HT, thermally

DOI: 10.1021/acsanm.9b01763
ACS Appl. Nano Mater. 2020, 3, 969–976

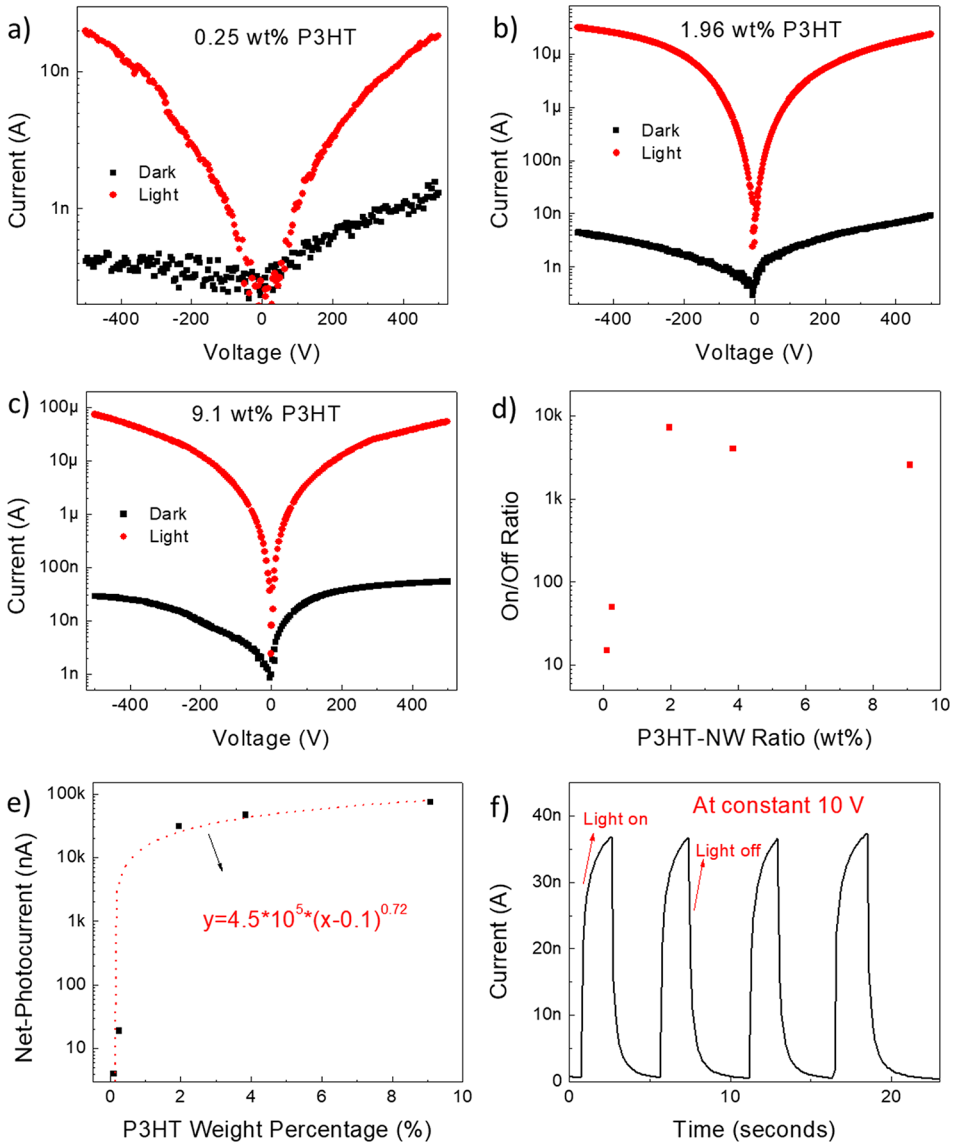

Figure 2. (a–c) *I*–*V* characteristics of vertical photodetectors using P3HT–polymer composites with 0.25, 1.96, and 9.1 wt % P3HT nanowires, respectively. The photodetectors have a device structure of ITO/P3HT nanowire–epoxy composite (50 μm)/In–Ga. All devices were measured in the dark (no light) and under light irradiation. A xenon lamp was used as the light source with a light intensity of 100 mW cm^{-2}. (d) Summary of on/off ratios and (e) net photocurrent at −500 V for photodetectors using P3HT nanowire–epoxy composites with different nanowire concentrations. The net-photocurrent data points can be simulated with a power law equation (dotted line and the inset in part e), suggesting a threshold concentration of 0.1 wt % to form continuous charge-transport networks in the P3HT nanowire–epoxy composites. (f) Transient responses with light on and off at constant 10 V from a photodetector with 1.96 wt % P3HT.

curable EPON resin, and UV-curable diacrylate are shown in Table S1.

P3HT Nanowire Synthesis and Composite Preparation. P3HT nanowires were synthesized following a modified literature procedure.[16,17] P3HT was first mixed with dichloromethane (DCM) at a concentration of 5 mg mL^{-1}. The mixture was sealed in a glass vial and placed on a 215 °C hot plate. In about 10 min, the solution temperature increased to 80 °C and P3HT became fully dissolved. The solution was then cooled at a rate of 1 °C min^{-1}, and the nanowire synthesis was completed when the solution reached room temperature. EPON Resin 862 and EPIKURE Curing Agent W were thoroughly mixed with a 100:26.3 weight ratio. P3HT nanowires were then added with different weight ratios, followed by removal of DCM at room temperature in a vacuum. DCM was used in this study because of its low boiling point, so it could be fully removed without using a high temperature, which can trigger curing of the epoxy resin. 3D printing ink was prepared by adding CNFs and mixing with a planetary centrifugal mixer (THINKY, ARE-310) for 2 min, followed by 30 s of degassing.

Material Characterizations. Scanning electron microscopy (SEM) was carried out with a JEOL 7401F microscope. Transmission electron microscopy (TEM) images were obtained using a JEM-ARM200cF microscope (cesium-corrected scanning/transmission electron microscope from JEOL) at 80 kV. The samples for TEM were dispersed on carbon/formva grids. X-ray diffraction (XRD) measurements were collected using a Scintag PAD-V θ-2θ diffractometer with Cu Kα radiation. Absorbance was measured with a UV–vis–near-IR spectrometer (Varian Cary 5000). Photoluminescence (PL) was measured using a 488 nm excitation laser with a confocal Raman system (Renishaw). The viscosity was measured by a Malvern Gemini 150 constant stress rheometer from 0 to 80 °C with a 1 °C min^{-1} heating rate.

3D Printing of Composite Structures. The ink was loaded into a syringe with a tip (1 mm) that was integrated with an air-pressure

DOI: 10.1021/acsanm.9b01763
ACS Appl. Nano Mater. 2020, 3, 969–976

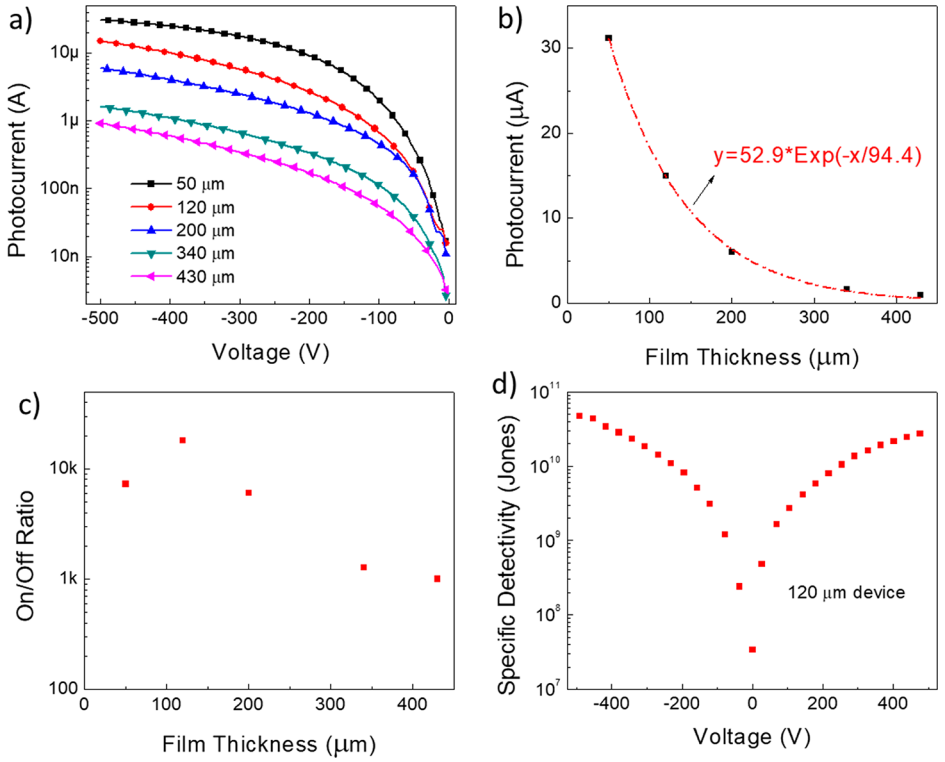

Figure 3. Study of the film thickness effect on photodetectors with 1.96 wt % P3HT nanowires: (a) $I-V$ characteristics; (b) photocurrent at −500 V versus film thickness. The photocurrent data points are fitted with an exponential decay equation (dotted line and the inset); (c) device on/off ratios versus film thickness; (d) specific detectivity versus voltage for the photodetector with a 120 μm composite film.

controller and a Zen Toolworks CNC 3D printer. Geometric codes were used to program the pathways of the tip.

Light Responses of Photodetectors. Device testing was carried out in ambient air with a humidity of 40−50%. The current−voltage ($I-V$) characteristics were measured with a Keithley 2410 sourcemeter and a xenon lamp (100 mW cm^{-2}).

RESULTS AND DISCUSSION

DCM is a relatively poor solvent for P3HT at room temperature (solubility <0.1 mg mL^{-1}; Figure S1). However, its solubility is greatly enhanced at high temperatures. As shown in Figure 1a−d, a clear orange P3HT/DCM (5 mg mL^{-1}) solution was obtained at 80 °C. The solution transformed into a translucent solution at 40−60 °C and a dark opaque mixture at 25 °C. The TEM and atomic force microscopy (AFM) images in parts e and f of Figure 1 both disclose the formation of P3HT nanowires in the P3HT/DCM mixture after cooling to 25 °C. The nanowires have diameters of ∼20 nm and lengths ranging from several hundred nanometers to ∼2 μm.

The P3HT nanowires in DCM were then mixed with an epoxy resin (EPON 862 base and EPIKURE W curing agent) or a UV-curable acrylic resin (bisphenol A ethoxylate diacrylate). DCM was removed in a vacuum chamber, and the remaining mixture was thermally or UV cured to obtain P3HT nanowire−polymer composites. One photograph of a cured sample with 1.96 wt % nanowires in epoxy is shown Figure 1g. The sample is about 5 mm wide, 8 cm long, and 2 mm thick and appears uniform in color throughout the sample. The SEM image in Figure 1h shows embedded and well-dispersed P3HT nanowires in the epoxy matrix. This result also indicates that the mixing and curing process did not cause physical damage to the nanowires. The XRD pattern in Figure 1i shows a peak at 2θ = 5.28°, confirming the ordered molecular assembly of the P3HT nanowires in the composite.[18] We further evaluated the optical properties of the P3HT nanowires and the nanowire−epoxy composite with absorption and PL spectroscopy. As shown in Figure 1j, the absorption spectrum shows a broad $\pi-\pi^*$ absorption from 400 to 700 nm. The PL spectrum shows a peak at ∼700 nm, correlating well with the onset of the absorption increase. The 3D-printed "FSU" patterns with P3HT nanowire−epoxy composites are shown in Figure 1k. Red PL is visible from the composites under a 365 nm UV-light source (Figure 1l).

To evaluate the photoresponses of P3HT nanowire−epoxy composites, we first fabricated photodetector devices on conductive indium−tin oxide (ITO) glass substrates with a vertical device architecture of ITO/P3HT nanowire−polymer composite/In−Ga. P3HT nanowires and epoxy resin were mixed with the desired weight ratios and drop-casted onto the ITO glass substrate. The mixture was thermally cured. The thickness of the resulting composite was about 50 μm. In−Ga was then applied as the top electrical contact to complete the photodetector fabrication. The device area for all photodetectors was 2 mm × 2 mm. The $I-V$ characteristics were obtained for each device in the dark and under light irradiation by sweeping the applied voltage from −500 to 500 V. The bias polarity is defined as positive when the ITO electrode is connected to the positive and In−Ga to the negative potential of the applied bias.

The $I-V$ characteristics for devices with the indicated P3HT concentrations are shown in Figure 2a−c. Overall, device currents in the dark and with light both increase with the applied bias and with increasing P3HT concentrations. Moreover, there are significant increases of the device currents

DOI: 10.1021/acsanm.9b01763
ACS Appl. Nano Mater. 2020, 3, 969−976

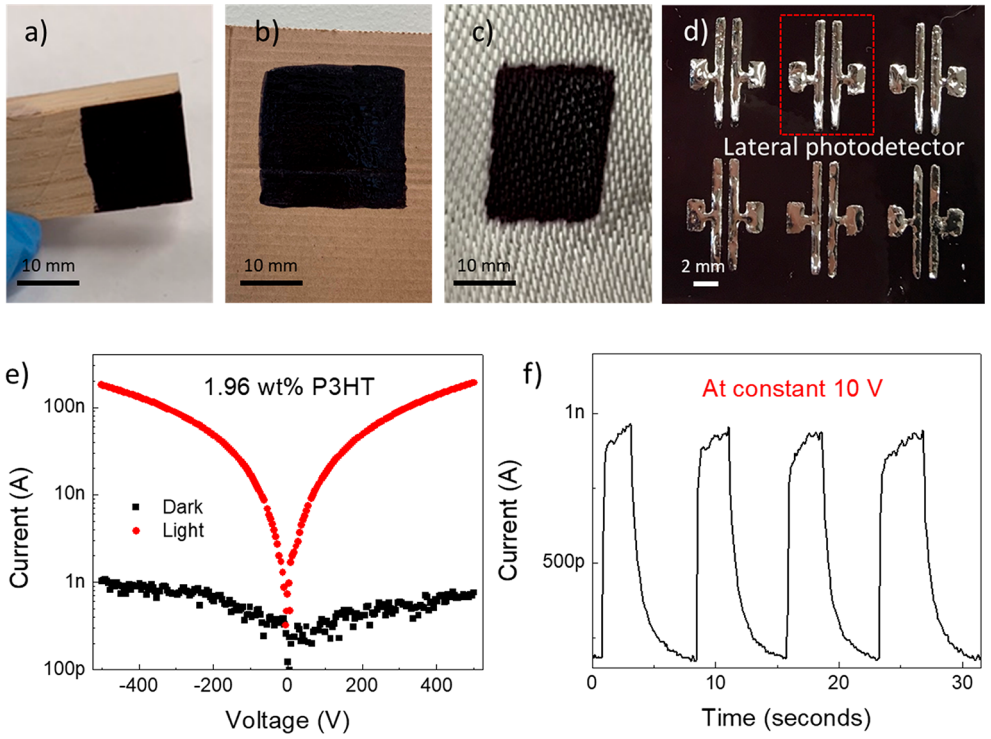

Figure 4. Painting of the P3HT nanowire–epoxy resin onto (a) a wood, (b) a cardboard, and (c) a glass fiber cloth surface. (d) Photograph showing a 2 × 3 array of lateral photodetectors fabricated on a cardboard surface. (e) *I*–*V* characteristics from −500 to +500 V. (f) Transient responses at 10 V of a lateral photodetector in part d using a composite containing 1.96 wt % P3HT nanowires.

when light is turned on for all composites with 0.25, 1.96, and 9.1 wt % P3HT nanowires, confirming the photosensitivity of the composites to the visible-light spectrum. All devices show a slightly higher dark current with a forward bias than with a reversed bias. This is caused by work function differences between the ITO (4.7 eV) and In–Ga (4.1–4.2 eV) electrodes.[19,20] Hole and electron injections become easier at a forward bias than at a reverse bias. Nonetheless, the device current becomes nearly identical for forward and reverse biases when light is turned on, suggesting that charge collection in the photoexcited nanowire–epoxy composites was dominated by a charge-drifting process under an external electric field. The energy barriers at the electrode–composite interfaces contribute a negligible role to the photocurrent likely because of the large thickness and high intrinsic resistance of the nanowire–epoxy composites.

A parameter of the on/off ratio is defined by the ratio of device currents at a specified bias with and without light irradiation. The maximum on/off ratios for devices with different P3HT concentrations appear at −400 to −500 V. As shown in Figure 2d, the on/off ratio starts to increase with increasing P3HT nanowire concentration, reaching the highest value of 7250 at 1.96 wt % P3HT and gradually decreasing afterward. The initial upgrowing trend is contributed by the fast increase of the photocurrent because more charge-transport pathways form in the composites with more P3HT nanowires. The latter decay comes from an increase of the dark current, which exceeds the gain on the photocurrent with a further increase of the P3HT nanowire concentration. Three devices for each P3HT nanowire concentration were fabricated from the same batch. Their on/off ratios were plotted in Figure S2, suggesting good repeatability of these devices.

The net photocurrent at −500 V by taking the difference of the device currents with and without light is plotted in Figure 2e versus the P3HT weight percentage. The value of the net photocurrent correlates with the charge-transport efficiency in the composites. The data were simulated with a power law equation (eq 1) according to percolation theory,[21] where m represents the P3HT nanowire concentration, m_c is the percolation threshold concentration, and α is a positive exponent. It is worth noting that a percolation threshold concentration of 0.1 wt % was obtained from the simulation. The very low threshold concentration is the result of using P3HT nanowires with high aspect ratios and uniformly dispersing the nanowires in the composites.[22]

$$\text{photocurrent} \propto (m - m_c)^{\alpha} \quad (1)$$

Figure 2f shows the transient responses with light on and off at a constant 10 V of the composite with 1.96 wt % P3HT. Overall, the photocurrent exhibits a fast rise and decay in the subsecond time frames when the light is both turned on and turned off, respectively. After that, much slower changes of the photocurrent are observed. The slow kinetics in the second stage are largely attributed to charge trapping and slow detrapping in the P3HT nanowire–polymer composites.[23]

The thickness effect on the photocurrent was also investigated for composites with 1.96 wt % P3HT nanowires. As shown in Figure 3a, the photocurrent shows a decreasing trend with increasing composite thicknesses. The photocurrent at −500 V was plotted versus composite thickness (Figure 3b). The data fit well to an exponential decay equation (eq 2), where d is the film thickness and τ is equal to 94.4 μm. Such a decay behavior is caused by the limited charge-carrier mobility/lifetime of P3HT and a decrease of the electric field with increasing composite film thicknesses.

DOI: 10.1021/acsanm.9b01763
ACS Appl. Nano Mater. 2020, 3, 969–976

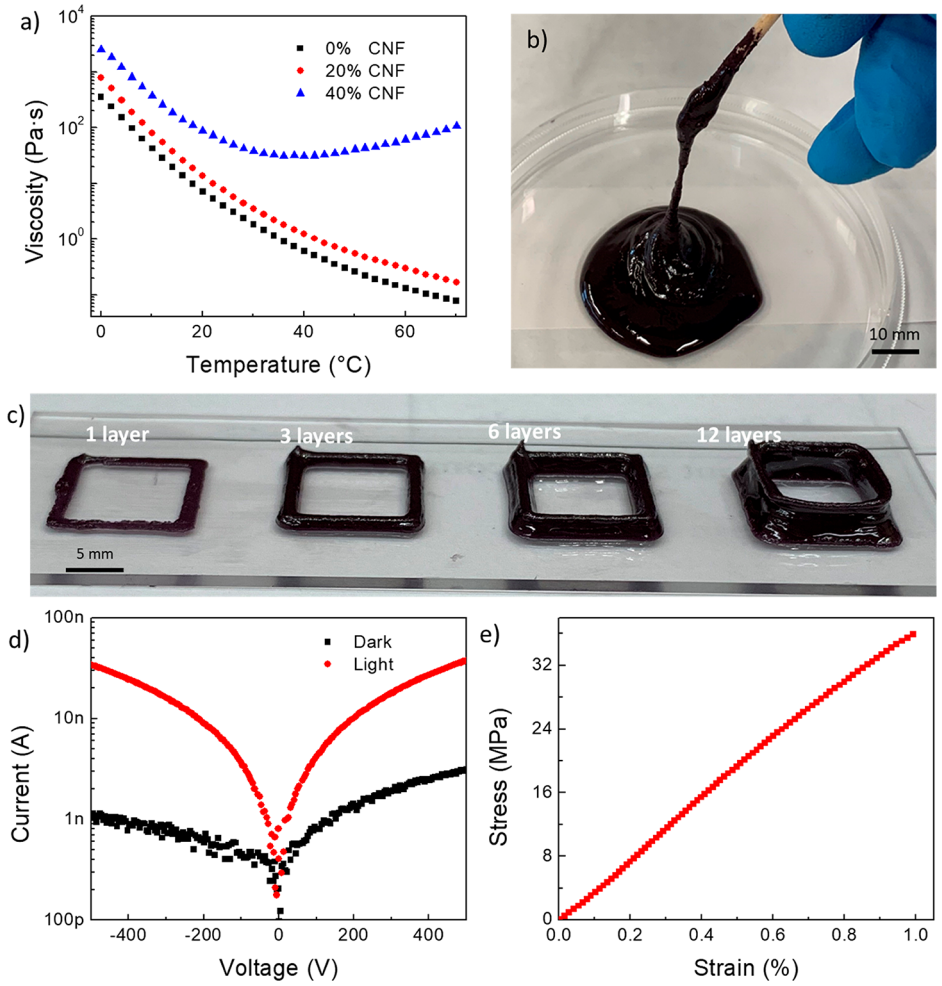

Figure 5. (a) Viscosity versus temperature characteristics of P3HT nanowire−epoxy inks showing the effect of adding CNFs to alter the ink rheological properties. (b) Photograph of a formulated ink with 1.0 wt % P3HT nanowires and 40 wt % CNFs in epoxy resin. (c) Photograph showing the progress of printing a 3D structure. (d) $I-V$ characteristics of a lateral photodetector fabricated on the surface of one 3D-printed P3HT nanowire (1 wt %)−epoxy (59 wt %)−CNF (40 wt %) composite sample. (e) Stress versus strain behavior of the 3D-printed composite in part d.

$$\text{photocurrent} \propto e^{-d/\tau} \tag{2}$$

The on/off ratio starts at 7250 for the device with a 50-μm-thick composite film and improves to 18025 with a 120-μm-thick film (Figure 3c). The increase of the on/off ratio from the 50-μm-thick device to the 120-μm-thick device is contributed by a large decrease in the dark current in the thicker device. The specific detectivity (D^*) of the device with a 120-μm-thick composite film is calculated according to eq 3, where J_{ph} is the photocurrent density, L_{light} is the incident light intensity, q is a unit of electric charge, and J_{dark} is the dark current density.[24,25] The maximum specific detectivity reaches 4.5×10^{10} Jones at −500 V (Figure 3d). The high values of the on/off ratios and specific detectivity are remarkable given the high thicknesses of the photoactive layers and fabrication simplicity of the photodetectors. Similar on/off ratios and specific detectivities were obtained in the literature; however, these devices had a 100× thinner photoactive layer that could not be used for any structural purpose and could suffer adhesion problems for engineering coatings.[24,25] The on/off ratios of the composite detectors decrease with a further increase of the film thicknesses due to a steady decrease of the photocurrent. Nonetheless, it maintains a value of 1000 even with a 430-μm-thick composite film.

$$D^* = \frac{J_{ph}/L_{light}}{\sqrt{2qJ_{dark}}} \tag{3}$$

In addition to thermally cured epoxy polymers, photocurable acrylic resins were also used as matrix polymers for the semiconducting nanowire composites. Parts a and b of Figure S3 show photographs of one 100-μm-thick composite sheet containing 1.96 wt % P3HT nanowires in the bisphenol A ethoxylate diacrylate (BAE) polymer. The composite was prepared by mixing P3HT nanowires with BAE resin and a photoinitiator, followed by a curing process with UV light at room temperature. In our experiments, we found that the maximum allowed thickness was about 1 mm for the 1.96 wt % P3HT nanowire composites. Thicker samples could not be fully cured with our current curing conditions because of the penetration depth limitation of UV light through the composites. Photodetectors with a 100-μm-thick composite were fabricated with the same vertical device structure as that of devices in Figure 2. The $I-V$ characteristics are shown in Figure S3c. The photocurrent is about 20 μA, and the dark

DOI: 10.1021/acsanm.9b01763
ACS Appl. Nano Mater. 2020, 3, 969−976

current is about 200 nA at −500 V, resulting in an on/off ratio of 100. The photocurrent from BAE composites is comparable to that of epoxy composites. However, the dark current from the BAE-based device is significantly higher, leading to an on/off value that is 100× worse than the epoxy-based device. The difference in the dark current can be caused by the different molecular interactions of the polymer matrixes and P3HT nanowires, leading to different defect densities on the nanowire surfaces.[26,27]

Epoxy and acrylic resins have been widely used for adhesives and surface coatings. Here, we evaluated the P3HT nanowire−epoxy composites as photoactive coatings. As shown in Figure 4a−c, the precursor ink was painted onto a wood, a cardboard, and a glass fiber cloth surface, respectively. Because all of the above substrates are insulating, photodetection characterizations with the previous vertical device structure are difficult. Therefore, lateral structure devices were used as shown in Figure 4d, where In−Ga electrodes were painted with a contact mask on the P3HT nanowire−epoxy composite surface and used as both the anode and cathode of the lateral photodetectors. The $I-V$ characteristics of one lateral photodetector are shown in Figure 4e. The device was fabricated on a cardboard substrate with a composite film containing 1.96 wt % P3HT nanowires. The distance of the two opposite In−Ga electrodes is 500 μm, and the electrode length is 8 mm. At ±500 V, the dark current is about 1 nA and the photocurrent is about 200 nA, resulting in an on/off ratio of 200 that is about 5 times lower than the vertical devices with a similar electrode distance (composite thickness). Such a result is likely due to the fact that the electric field mostly concentrates near the surface area of the composite in the lateral photodetectors, and only charge carriers generated close to the surface can be collected. The transient response of the lateral photodetector was tested at 10 V (Figure 4f). Like the vertical device in Figure 2f, the device current starts with a fast rise or drop, followed by a slower rate of change when the light is switched on or off.

The P3HT nanowire−epoxy composites were also applied to printing 3D photodetectors. Semiconducting polymers that include P3HT are typically processed using solution-based spin-coating, inkjet-printing, or screen-printing processes into thin films with thicknesses from sub-100 nm to a few micrometers. 3D-printed P3HT photodetectors were first reported by Park et al. by depositing P3HT thin films on top of 3D passive structures using a modified inkjet-printing process.[28] In contrast, using semiconducting nanowire−epoxy composites in this current work enables tuning of the rheological properties of the printing inks, allowing the direct printing of 3D monolithic structures that can sense incident light intensities among all surfaces of the 3D structures.

In 3D printing, a delicate balance must be struck; it is critical that the printed structures do not collapse under their own weight between deposition from the nozzle head and final curing. However, the material must have a low enough viscosity that it can be pushed through the nozzle head. To realize this goal, we reformulated the P3HT nanowire−epoxy inks by adding CNFs because our original inks were not viscous enough for 3D printing. The rheological properties of the P3HT nanowire−epoxy−CNF inks are shown in Figure 5a. For the pristine ink without added CNFs, its viscosity decreases with rising temperature. Adding 20 wt % CNFs enhances the viscosity; however, the same trend of viscosity decay with temperature is observed. When the CNF concentration is increased to 40 wt %, the viscosity shows a monotonic decrease from 0 to 32 °C; however, it starts to increase after 32 °C. This property is beneficial for preserving the original shapes of the 3D-printed structures during the postcuring process.

The photograph in Figure 5b manifests the high viscosity of the 3D-printing ink with 40% CNFs. The ink was extruded from a pressurized syringe with a 1-mm-diameter tip. The real-time printing process to fabricate a 3D square structure can be seen in a video in the Supporting Information. The photographs in Figure 5c show the progress of printing when 1 layer, 3 layers, 6 layers, and 12 layers were just completed, respectively. Curing took place at room temperature for 12 h and then at 100 °C for another 12 h. Lateral photodetectors were fabricated with the same configuration as that of the devices in Figure 4d on the 3D-printed P3HT nanowire−epoxy−CNF composite. The photoresponses are characterized in Figure 5d. A dark current of about 1 nA and a photocurrent of about 34 nA were obtained at −500 V, leading to an on/off ratio of 34. Tensile testing was used to evaluate the mechanical properties of the 3D-printed composite. According to Figure 5e, the composite can sustain about 1% strain before failure and exhibits a Young's modulus of about 4 GPa and an ultimate strength of 36 MPa. These values are encouraging first steps toward applying such photoactive composites for 3D-printed engineering structures.

CONCLUSION

We have developed P3HT nanowire−epoxy or acrylic resin inks that are cured with heat or UV light to form rigid photoactive composites capable of converting visible light to an electric current signal. The high aspect ratios of the P3HT nanowires enable the formation of percolated P3HT networks for charge-carrier collection at a very low P3HT concentration of 0.1 wt %. Light detection with a high on/off ratio of 18025 is achieved with composites containing 1.96 wt % P3HT nanowires. The composite ink can be used as paints to create light sensors in the form of photoactive coatings on various surfaces. The ink can also be modified for 3D-printed light sensors in the form of rigid photoactive structures that have a mechanical modulus and strength comparable to those of common structural polymers and composites. The strategy of using semiconducting nanowire−polymer composites can be further explored for the creation of multifunctional composite sensors that have the optoelectronic properties of conventional semiconductors and the mechanical and manufacturing advantages of polymer composites.

ASSOCIATED CONTENT

Supporting Information

The Supporting Information is available free of charge at https://pubs.acs.org/doi/10.1021/acsanm.9b01763.

Chemical structures of P3HT, thermally curable EPON resin, and UV-curable diacrylate, photograph of a mixture of 1 mg of P3HT and 10 mL of DCM at room temperature, statistic plots of on/off ratios for devices with different P3HT nanowire concentrations, and photographs and light-responsive measurements of P3HT nanowire composites in a UV-cured acrylic polymer (PDF)

Real-time video recording of the 3D-printing progression to fabricate 3D photoactive structures (AVI)

DOI: 10.1021/acsanm.9b01763
ACS Appl. Nano Mater. 2020, 3, 969−976

AUTHOR INFORMATION

Corresponding Author

*Email: zyu@fsu.edu.

ORCID

Zhibin Yu: 0000-0002-4630-4363

Author Contributions

The manuscript was written through contributions of all authors. All authors have given approval to the final version of the manuscript.

Notes

The authors declare no competing financial interest.

ACKNOWLEDGMENTS

Z.Y. is thankful for financial support by the National Science Foundation under Award ECCS-1609032 and by the Air Force Office of Scientific Research (AFOSR) under Award FA9550-16-1-0124. TEM work was performed at the National High Magnetic Field Laboratory, which is supported by National Science Foundation Cooperative Agreement DMR-1644779 and the State of Florida. S.R. and D.B. acknowledge support by NSF CREST Center Award 1735968. We thank Dr. Nam Nguyen for technical assistance in 3D printing the polymer composites.

REFERENCES

(1) Friedrich, K.; Almajid, A. A. Manufacturing Aspects of Advanced Polymer Composites for Automotive Applications. *Appl. Compos. Mater.* **2013**, *20* (2), 107−128.

(2) Bakis, C. E.; Bank, L. C.; Brown, V. L.; Cosenza, E.; Davalos, J. F.; Lesko, J. J.; Machida, A.; Rizkalla, S. H.; Triantafillou, T. C. Fiber-reinforced polymer composites for construction-state-of-the-art review. *J. Compos. Constr.* **2002**, *6* (2), 73−87.

(3) Mangalgiri, P. D. Composite materials for aerospace applications. *Bull. Mater. Sci.* **1999**, *22* (3), 657−664.

(4) Wang, X.; Jiang, M.; Zhou, Z. W.; Gou, J. H.; Hui, D. 3D printing of polymer matrix composites: A review and prospective. *Composites, Part B* **2017**, *110*, 442−458.

(5) Ligon, S. C.; Liska, R.; Stampfl, J.; Gurr, M.; Mulhaupt, R. Polymers for 3D Printing and Customized Additive Manufacturing. *Chem. Rev.* **2017**, *117* (15), 10212−10290.

(6) Do, A. V.; Khorsand, B.; Geary, S. M.; Salem, A. K. 3D Printing of Scaffolds for Tissue Regeneration Applications. *Adv. Healthcare Mater.* **2015**, *4* (12), 1742−1762.

(7) Gonzalez, C.; Vilatela, J. J.; Molina-Aldareguia, J. M.; Lopes, C. S.; LLorca, J. Structural composites for multifunctional applications: Current challenges and future trends. *Prog. Mater. Sci.* **2017**, *89*, 194−251.

(8) Gu, H. B.; Ma, C.; Gu, J. W.; Guo, J.; Yan, X. R.; Huang, J. N.; Zhang, Q. Y.; Guo, Z. H. An overview of multifunctional epoxy nanocomposites. *J. Mater. Chem. C* **2016**, *4* (25), 5890−5906.

(9) Alarifi, I. M.; Alharbi, A.; Khan, W. S.; Asmatulu, R. Carbonized electrospun polyacrylonitrile nanofibers as highly sensitive sensors in structural health monitoring of composite structures. *J. Appl. Polym. Sci.* **2016**, *133* (13), 43235.

(10) Qing, X. P.; Beard, S. J.; Kumar, A.; Ooi, T. K.; Chang, F. K. Built-in sensor network for structural health monitoring of composite structure. *J. Intell. Mater. Syst. Struct.* **2007**, *18* (1), 39−49.

(11) Olawale, D. O.; Dickens, T.; Sullivan, W. G.; Okoli, O. I.; Sobanjo, J. O.; Wang, B. Progress in triboluminescence-based smart optical sensor system. *J. Lumin.* **2011**, *131* (7), 1407−1418.

(12) Kalsoom, U.; Nesterenko, P. N.; Paull, B. Recent developments in 3D printable composite materials. *RSC Adv.* **2016**, *6* (65), 60355−60371.

(13) Barlian, A. A.; Park, W. T.; Mallon, J. R.; Rastegar, A. J.; Pruitt, B. L. Review: Semiconductor Piezoresistance for Microsystems. *Proc. IEEE* **2009**, *97* (3), 513−552.

(14) Zhang, X.; Yu, Z. B.; Wang, C.; Zarrouk, D.; Seo, J. W. T.; Cheng, J. C.; Buchan, A. D.; Takei, K.; Zhao, Y.; Ager, J. W.; Zhang, J. J.; Hettick, M.; Hersam, M. C.; Pisano, A. P.; Fearing, R. S.; Javey, A. Photoactuators and motors based on carbon nanotubes with selective chirality distributions. *Nat. Commun.* **2014**, *5*, 2983.

(15) Dang, M. T.; Hirsch, L.; Wantz, G. P3HT:PCBM, Best Seller in Polymer Photovoltaic Research. *Adv. Mater.* **2011**, *23* (31), 3597−3602.

(16) Kim, H. J.; Sim, K.; Thukral, A.; Yu, C. J. Rubbery electronics and sensors from intrinsically stretchable elastomeric composites of semiconductors and conductors. *Sci. Adv.* **2017**, *3* (9), e1701114.

(17) Lee, Y.; Oh, J. Y.; Son, S. Y.; Park, T.; Jeong, U. Effects of Regioregularity and Molecular Weight on the Growth of Polythiophene Nanofibrils and Mixes of Short and Long Nanofibrils To Enhance the Hole Transport. *ACS Appl. Mater. Interfaces* **2015**, *7* (50), 27694−27702.

(18) Colle, R.; Grosso, G.; Ronzani, A.; Zicovich-Wilson, C. M. Structure and X-ray spectrum of crystalline poly(3-hexylthiophene) from DFT-van der Waals calculations. *Phys. Status Solidi B* **2011**, *248* (6), 1360−1368.

(19) Chiechi, R. C.; Weiss, E. A.; Dickey, M. D.; Whitesides, G. M. Eutectic gallium-indium (EGaIn): A moldable liquid metal for electrical characterization of self-assembled monolayers. *Angew. Chem., Int. Ed.* **2008**, *47* (1), 142−144.

(20) Ran, C. X.; Xi, J.; Gao, W. Y.; Yuan, F.; Lei, T.; Jiao, B.; Hou, X.; Wu, Z. X. Bilateral Interface Engineering toward Efficient 2D-3D Bulk Heterojunction Tin Halide Lead-Free Perovskite Solar Cells. *Acs Energy Lett.* **2018**, *3* (3), 713.

(21) Garboczi, E. J.; Snyder, K. A.; Douglas, J. F.; Thorpe, M. F. Geometrical Percolation-Threshold of Overlapping Ellipsoids. *Phys. Rev. E: Stat. Phys., Plasmas, Fluids, Relat. Interdiscip. Top.* **1995**, *52* (1), 819−828.

(22) Ramasubramaniam, R.; Chen, J.; Liu, H. Y. Homogeneous carbon nanotube/polymer composites for electrical applications. *Appl. Phys. Lett.* **2003**, *83* (14), 2928−2930.

(23) Li, Z.; McNeill, C. R. Transient photocurrent measurements of PCDTBT:PC(70)BM and PCPDTBT:PC(70)BM Solar Cells: Evidence for charge trapping in efficient polymer/fullerene blends. *J. Appl. Phys.* **2011**, *109* (7), 074513.

(24) Baeg, K. J.; Binda, M.; Natali, D.; Caironi, M.; Noh, Y. Y. Organic Light Detectors: Photodiodes and Phototransistors. *Adv. Mater.* **2013**, *25* (31), 4267−4295.

(25) Gong, X.; Tong, M. H.; Xia, Y. J.; Cai, W. Z.; Moon, J. S.; Cao, Y.; Yu, G.; Shieh, C. L.; Nilsson, B.; Heeger, A. J. High-Detectivity Polymer Photodetectors with Spectral Response from 300 to 1450 nm. *Science* **2009**, *325* (5948), 1665−1667.

(26) Perez, M. D.; Borek, C.; Forrest, S. R.; Thompson, M. E. Molecular and Morphological Influences on the Open Circuit Voltages of Organic Photovoltaic Devices. *J. Am. Chem. Soc.* **2009**, *131* (26), 9281−9286.

(27) Wang, D. W.; Chang, Y. L.; Wang, Q.; Cao, J.; Farmer, D. B.; Gordon, R. G.; Dai, H. J. Surface chemistry and electrical properties of germanium nanowires. *J. Am. Chem. Soc.* **2004**, *126* (37), 11602−11611.

(28) Park, S. H.; Su, R. T.; Jeong, J.; Guo, S. Z.; Qiu, K. Y.; Joung, D.; Meng, F. B.; McAlpine, M. C. 3D Printed Polymer Photodetectors. *Adv. Mater.* **2018**, *30* (40), 1803980.

DOI: 10.1021/acsanm.9b01763
ACS Appl. Nano Mater. 2020, 3, 969−976